Creation of Rift Valley Fever Viruses with Four-Segmented Genomes Reveals Flexibility in Bunyavirus Genome Packaging

Paul J. Wichgers Schreur,[a] Nadia Oreshkova,[a,b] Rob J. M. Moormann,[a,b] Jeroen Kortekaas[a]

Department of Virology, Central Veterinary Institute, part of Wageningen University and Research Centre, Lelystad, The Netherlands[a]; Department of Infectious Diseases and Immunology, Virology Division, Faculty of Veterinary Medicine, Utrecht University, Utrecht, The Netherlands[b]

ABSTRACT

Bunyavirus genomes comprise a small (S), a medium (M), and a large (L) RNA segment of negative polarity. Although the untranslated regions have been shown to comprise signals required for transcription, replication, and encapsidation, the mechanisms that drive the packaging of at least one S, M, and L segment into a single virion to generate infectious virus are largely unknown. One of the most important members of the *Bunyaviridae* family that causes devastating disease in ruminants and occasionally humans is the Rift Valley fever virus (RVFV). We studied the flexibility of RVFV genome packaging by splitting the glycoprotein precursor gene, encoding the (NSm)GnGc polyprotein, into two individual genes encoding either (NSm)Gn or Gc. Using reverse genetics, six viruses with a segmented glycoprotein precursor gene were rescued, varying from a virus comprising two S-type segments in the absence of an M-type segment to a virus consisting of four segments (RVFV-4s), of which three are M-type. Despite that all virus variants were able to grow in mammalian cell lines, they were unable to spread efficiently in cells of mosquito origin. Moreover, *in vivo* studies demonstrated that RVFV-4s is unable to cause disseminated infection and disease in mice, even in the presence of the main virulence factor NSs, but induced a protective immune response against a lethal challenge with wild-type virus. In summary, splitting bunyavirus glycoprotein precursor genes provides new opportunities to study bunyavirus genome packaging and offers new methods to develop next-generation live-attenuated bunyavirus vaccines.

IMPORTANCE

Rift Valley fever virus (RVFV) causes devastating disease in ruminants and occasionally humans. Virions capable of productive infection comprise at least one copy of the small (S), medium (M), and large (L) RNA genome segments. The M segment encodes a glycoprotein precursor (GPC) protein that is cotranslationally cleaved into Gn and Gc, which are required for virus entry and fusion. We studied the flexibility of RVFV genome packaging and developed experimental live-attenuated vaccines by applying a unique strategy based on the splitting of the GnGc open reading frame. Several RVFV variants, varying from viruses comprising two S-type segments to viruses consisting of four segments (RVFV-4s), of which three are M-type, could be rescued and were shown to induce a rapid protective immune response. Altogether, the segmentation of bunyavirus GPCs provides a new method for studying bunyavirus genome packaging and facilitates the development of novel live-attenuated bunyavirus vaccines.

A n important member of the *Bunyaviridae* family, belonging to the *Phlebovirus* genus and causing devastating disease in ruminants and occasionally humans, is the Rift Valley fever virus (RVFV). RVFV is endemic to the African continent, Madagascar, the Comoros Islands, Mayotte and the Arabian Peninsula and is transmitted among livestock by *Aedine* and *Culicine* mosquitoes (1). RVFV epizootics are characterized by near simultaneous abortions, particularly among sheep, and high mortality among young animals below the age of 2 weeks. Humans can be infected via mosquito bite, but more commonly via contact with bodily fluids released during slaughtering of viremic animals. The majority of infected humans display a transient febrile illness, whereas a small percentage of individuals develop complications such as retinal lesions, hepatic disease with hemorrhagic fever or delayed-onset encephalitis.

RVFV comprises, like all bunyaviruses, a trisegmented single-stranded RNA genome of negative polarity (2). The small (S) genome segment encodes the nucleocapsid (N) protein in genomic-sense orientation and a nonstructural protein, named NSs, in antigenomic-sense orientation. The N protein encapsidates the viral RNA to form ribonucleoprotein complexes (RNPs) and the NSs protein functions as an antagonist of host innate immune responses and is considered the major virulence factor (3–7). The

medium-size (M) segment encodes the viral structural glycoproteins Gn and Gc, and a nonstructural protein referred to as NSm. NSm is described to have an antiapoptotic function (8, 9) and to be involved in virus dissemination from the mosquito midgut (10). In addition, the M segment encodes a 78-kDa protein of unknown function that is incorporated in virions of virus replicating in the mosquito vector (11). The proteins encoded by the M-segment are produced from a glycoprotein precursor (GPC) which is cotranslationally cleaved by as-yet-unknown host proteases (12–14). The large (L) genome segment encodes the viral
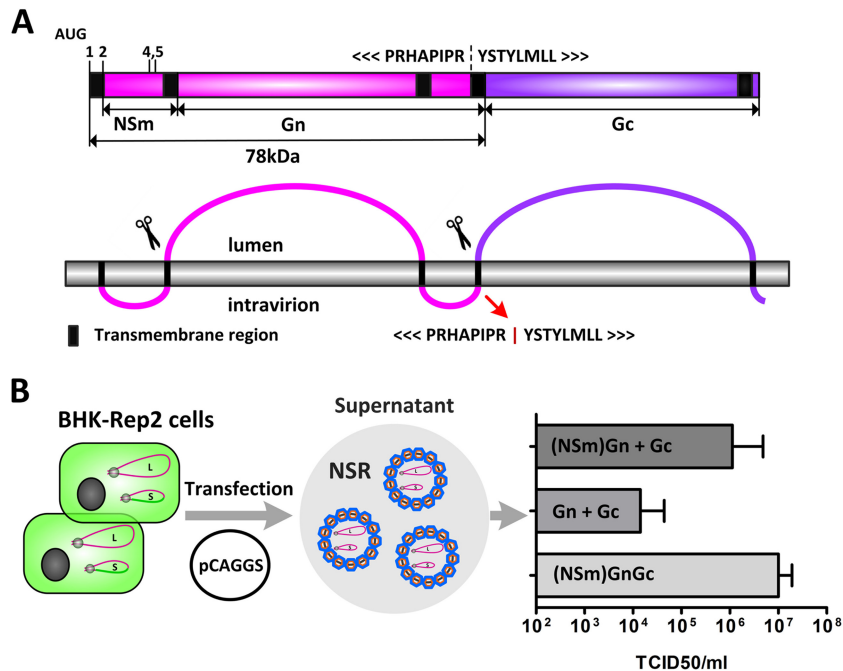
FIG 1 Effect of GPC segmentation on NSR production. (A) Schematic presentation of M-segment-encoded proteins and protein processing. The dashed line and the red arrow indicate the position where the Gn and Gc coding sequences were separated. (B) BHK-Rep2 cells, stably maintaining replicating RVFV L and S$_{eGFP}$ genome segments were transfected with pCAGGS expression plasmids encoding Gn, NSmGn, Gc, or NSmGnGc. One day posttransfection, the levels of NSR progeny in the supernatant were determined by titration on BHK-21 cells. The bars represent means and standard errors of three experiments.

RNA-dependent RNA polymerase responsible for transcription and genome replication.

The noncoding or untranslated regions (UTRs) of bunyavirus genome segments contain signals required for the initiation and termination of transcription, replication, encapsidation, and packaging (15–22). The 3′ and 5′ termini of each segment contain genus-, virus-, and segment-specific nucleotides and the inverted complementarity of these regions facilitates the formation of pan-handle structures (2, 16). To generate infectious virus, at least one S, M, and L segment should be packaged into a single virion. The polymerase and the N protein are proposed to interact with the cytosolic tail of the Gn protein, thereby ensuring incorporation of RNPs into budding virions (22). Whether the different genome segments (S, M, and L) are selectively or randomly packaged into virions is not known. It was previously proposed that the M segment plays a pivotal role in the copackaging of the L and S segments (20). However, we and others have demonstrated that the M segment is not required for the packaging of L and S genome segments into RVFV replicon particles (23, 24), and a two-segmented RVFV that expresses the Gn and Gc genes from the NSs location of the S segment was shown to be viable without an M-type genome segment (25). Altogether, these studies have provided important new insights into bunyavirus packaging; however, they also made clear that many questions on this topic remain to be answered.

To expand our knowledge on bunyavirus packaging, we studied the flexibility in RVFV genome packaging using a novel strategy that is based on the splitting of the GPC gene into two individual genes encoding either (NSm)Gn or Gc. The results of our study show that RVFV is able to stably maintain four, instead of three genome segments.

MATERIALS AND METHODS

Ethics statement. The animal experiment was conducted in accordance with the Dutch Law on Animal Experiments (Wod, ID number BWBR0003081) and approved by the Animal Ethics Committee of the Central Veterinary Institute (permit 2013050).

Cells and viruses. BHK, BHK-Rep2 (23), BSR-T7/5 (26), and C6/36 cells were maintained as described previously (23). All RVFV variants described in the present study contain the RVFV strain 35/74 genetic backbone (23, 27). Virus titers are expressed as 50% tissue culture infective doses (TCID$_{50}$)/ml and were determined using the Spearman-Kärber algorithm.

Plasmids. To transiently express genes of interest, pCAGGS plasmids were used. Genome segments were transcribed from pUC57 plasmids from a minimal T7 promoter. All plasmids were constructed using standard cloning techniques with the additional help of gene synthesis (Gen-Script Corp., NJ). Detailed information about the plasmids is summarized in Table S1 in the supplemental material and can be provided on request. Plasmids containing half of the GPC gene, either encoding (NSm)Gn or Gc, were segmented at the tyrosine (Y)-675 codon of NSmGnGc (Fig. 1A), without any nucleotide overlap. (Y)-675 is predicted to be the first amino acid of the signal sequence of Gc (13, 14).

Production of RVFV replicon particles. BHK-Rep2 cells were seeded in six-well plates and after overnight incubation transfected with a total of 3 μg of pCAGGS expression plasmid using JetPEI transfection reagents (Polyplus-Transfection SA, Illkirch, France) according to the manufacturer's instructions. At 1 day posttransfection, the supernatants were harvested and titrated on BHK cells.

Rescue experiments. BSR-T7/5 cells were seeded in six-well plates (500.000 cells/well) and after overnight incubation infected for 2 h with fowlpox T7 (FP-T7) (28). Subsequently, medium was refreshed and cells were transfected with a total of 3 μg of pUC57 transcription plasmids per well using JetPEI transfection reagents according to the manufacturer's instructions. At 3 to 5 days posttransfection, the supernatants were col-

lected and used to infect freshly seeded BSR-T7/5 cells. Viral rescue was visualized using immunofluorescence assays (IFAs).

Immunofluorescence. IFAs were performed as previously described with some modifications (29). Briefly, infected cell monolayers were fixed with 4% (wt/vol) paraformaldehyde (15 min) and permeabilized with cold methanol (5 min). Blocking (30 min) and antibody incubations (1 h at 37°C) were subsequently performed in phosphate-buffered saline (PBS) supplemented with 5% horse serum. To detect Gn expression, monoclonal antibody 4-39-cc was used (30) in combination with a Texas Red-conjugated secondary antibody (Abcam, Cambridge, United Kingdom), and to detect Gc expression, a polyclonal rabbit antibody was used (31) in combination with an Alexa Fluor 350-conjugated secondary antibody (Life Technologies, Bleiswijk, The Netherlands). Between antibody incubations, the cells were washed three times with washing buffer (PBS, 0.05% [vol/vol] Tween 20). Antibody binding was visualized using an AMG EVOS-FL fluorescence microscope.

Northern blotting. Northern blotting was performed using a DIG Northern starter kit (Roche, Woerden, The Netherlands) in combination with the Northern-Max-Gly kit (Ambion, Austin, TX) as previously described (23). Primers used for the generation of the RNA probes are listed in Table S2 in the supplemental material. Viral RNA was isolated using TRIzol LS (Sigma-Aldrich, MO) in combination with the Direct-Zol RNA miniprep kit (Zymo Research, CA) according to the manufacturer's instructions.

Western blotting. Infected BSR cells in six-well plates were washed with PBS and subsequently lysed in 500 µl of lysis buffer (100 mM Tris-HCl [pH 6.8], 4% sodium dodecyl sulfate, 20% glycerol, 200 mM dithiothreitol, 0.2% bromophenol blue, and 25 U/ml Benzonase [Novagen]). After separation in 4 to 12% NuPAGE Bis-Tris gels (Invitrogen), proteins were blotted onto nitrocellulose membranes. Western blot analysis was performed with a rabbit α-Gn peptide antiserum (32), a rabbit α-Gc peptide antiserum (32), and a monoclonal antibody against N (F1D11) (33). Horseradish peroxidase-conjugated secondary antibodies were used according the manufacturer's instructions (Dako). The membrane was blocked with PBS containing 0.05% Tween 20 (vol/vol) and 5% (wt/vol) Elk (Campina). Binding was visualized using ECL substrate (GE Healthcare).

Animal experiments. (i) *In vivo* **dissemination of RVFV-LMMS$_{NSs}$.** Nine-week-old female BALB/cAnCrl mice (Charles River Laboratories) were divided in two groups of 16 mice and one group of 10 mice, kept in type III filter top cages under BSL-3 conditions, and allowed to acclimatize for 6 days. At day 0, the two groups of 16 mice were infected intraperitoneally (0.1 ml) with either a low ($10^{3.8}$ TCID$_{50}$) or a high ($10^{5.8}$ TCID$_{50}$) dose of RVFV-LMMS$_{NSs}$. As a positive control, a group of 10 mice was infected with a low ($10^{2.8}$ TCID$_{50}$) dose of authentic RVFV strain 35/74. Mice were observed daily, and at days 1, 4, 8, and 11 postinfection four mice were euthanized from the groups infected with RVFV-LMMS$_{NSs}$. Viral dissemination in the livers and brains was evaluated by quantitative reverse transcription-PCR (qRT-PCR) as described previously (34).

(ii) Vaccination-challenge experiment. Six-week-old female BALB/cAnCrl mice (Charles River Laboratories) were divided into four groups of 10 mice, kept in type III filter top cages under BSL-3 conditions, and allowed to acclimatize for 6 days. At day 0, mice were vaccinated intramuscularly (thigh muscle) with either medium (Mock), NSR-Gn (29) ($10^{5.8}$ TCID$_{50}$), RVFV-LMMS$_{eGFP}$ ($10^{5.8}$ TCID$_{50}$), or RVFV-LMMS$_{delNSs}$ ($10^{5.8}$ TCID$_{50}$) in 50 µl. Mice were observed daily, and at 3 weeks postvaccination mice were challenged intraperitoneally with $10^{2.8}$ TCID$_{50}$ of RVFV strain 35/74 in 0.1 ml of medium. One day prior to challenge, RVFV-specific neutralization titers in sera were determined as described previously (23) using RVFV-LMMS$_{eGFP}$ as the antigen. Virus dissemination to livers and brains was evaluated by qRT-PCR as described previously (34).

Statistical analysis. Data were analyzed and visualized using GraphPad 5.0 software.

RESULTS

Splitting of the RVFV GPC gene does not abrogate the functionality of Gn and Gc. Bunyavirus M segments encode GPCs that are proteolytically cleaved into proteins that function in receptor binding and fusion. To evaluate whether proteolytic processing of the RVFV GPC is a prerequisite for the functionality of Gn and Gc, we constructed expression plasmids encoding either (NSm)Gn or Gc and evaluated their ability to facilitate production of RVFV replicon particles (also referred to as nonspreading RVFV [NSR] [23]). The GPC was split at the tyrosine (Y)-675 codon, which is predicted to be the first amino acid of the signal sequence of Gc (Fig. 1A) (13, 14). Briefly, BHK cells stably maintaining replicating L and S$_{eGFP}$ genome segments (BHK-Rep2) were cotransfected with pCAGGS-(NSm)Gn and pCAGGS-Gc, and 1 day later the supernatants were collected and titrated (Fig. 1B). As a positive control, BHK-Rep2 cells were transfected with pCAGGS-M, which encodes wild-type NSmGnGc (23). Cotransfection of pCAGGS-Gn and pCAGGS-Gc resulted in average NSR particles of 10^4 TCID$_{50}$/ml, whereas cotransfection of pCAGGS-NSmGn and pCAGGS-Gc resulted in an average NSR particle production of 10^6 TCID$_{50}$/ml, nearly reaching the level generally obtained after transfection with pCAGGS-M. These results show that splitting of the GPC gene does not abrogate Gn and Gc functionality.

Rescue of RVFV with a segmented GPC gene. After demonstrating that RVFV L and S genome segments can efficiently be packaged into infectious replicon particles using the NSmGn and Gc expression plasmids, we investigated, by reverse genetics, whether virus expressing NSmGn and Gc from separate genome segments is viable. The transcription plasmids pUC57-L, pUC57-M-Gc, and pUC57-S-NSmGn were used for the rescue of viruses that express NSmGn from the NSs location of the S segment, and transcription plasmids pUC57-L, pUC57-M-NSmGn, and pUC57-S-Gc were used for the rescue of viruses that express Gc from the NSs location. We have thus far not been able to rescue viruses that express NSmGn from the NSs location of the S segment and Gc from the M segment. However, a virus that expresses Gc from the S segment and NSmGn from the M segment could be rescued, as evidenced by immunofluorescence assay (IFA) and Northern blotting (Fig. 2 and 3). The virus, hereafter referred to as RVFV-LMS-split, was able to grow to 10^6 TCID$_{50}$/ml in BSR cells (Fig. 4) and induced an RVFV-specific cytopathic effect (CPE) about 1 day later than wild-type virus. The successful rescue of the LMS-split virus demonstrates that Gn and Gc are fully functional when expressed from separate genome segments.

RVFV is able to maintain two S-type genome segments. The finding that Gn and Gc do not require processing as a GPC protein to produce progeny virus provided new opportunities to study the dynamics of RVFV genome packaging. In a first experiment, we investigated whether RVFV is able to package two S-type genome segments in the absence of an M-type genome segment. Rescue experiments were performed with transcription plasmids pUC57-L, pUC57-S-Gc, and pUC57-S-NSmGn. In this situation, both NSmGn and Gc are expressed from the NSs gene location of an S segment. In several attempts, the presence of infectious double S-segment virus, as evidenced by IFA and Northern blotting, could be confirmed (Fig. 2 and 3). The virus, hereafter referred to as RVFV-LSS, is able to grow up to titers of 10^5 TCID$_{50}$/ml in BSR cells (Fig. 4), which is ~10 times lower than what was observed with RVFV-LMS-split. Compared to wild-type virus, CPE result-
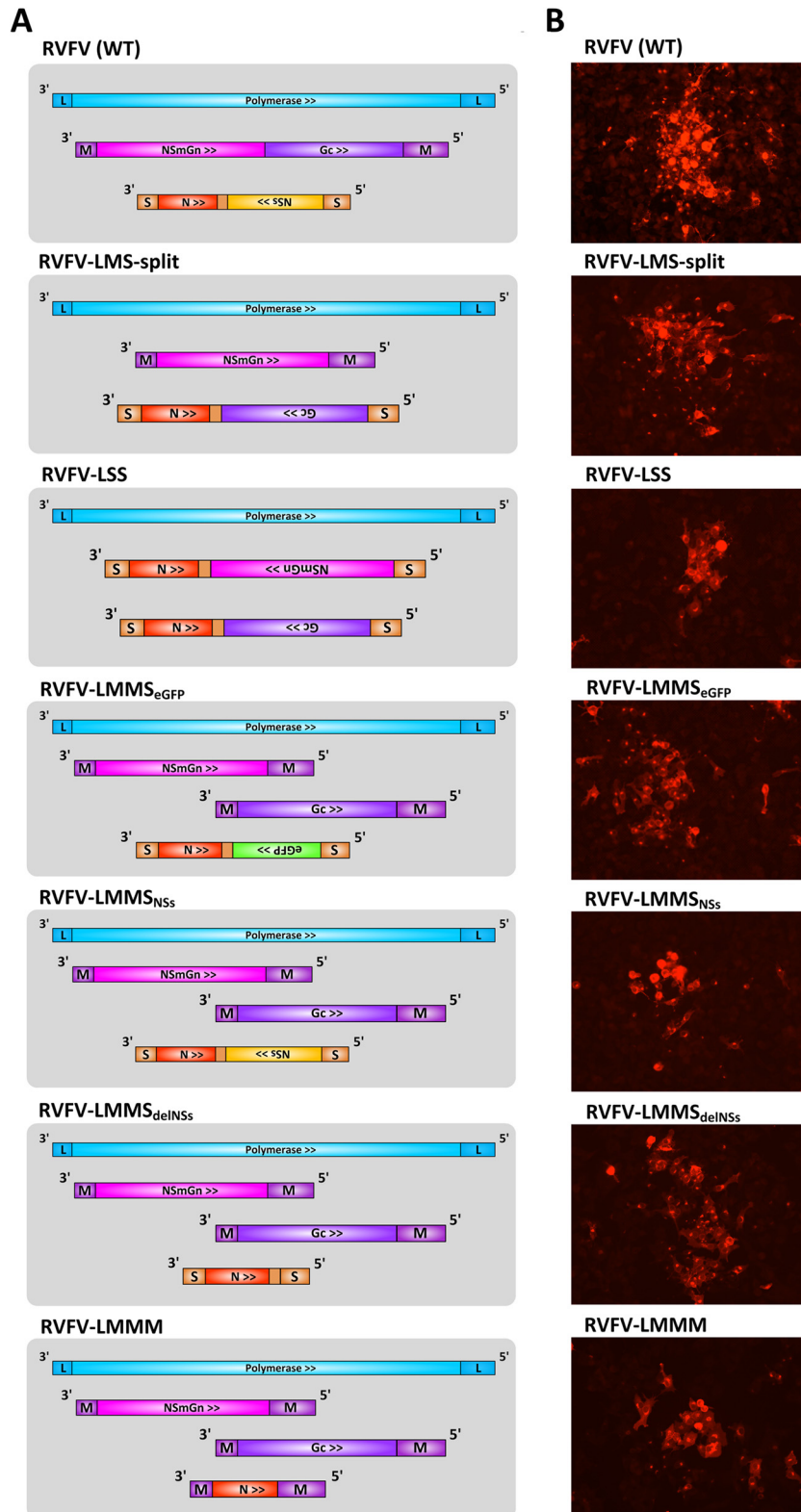
FIG 2 Rescue of RVFV variants with segmented GPC genes. (A) Schematic presentation of RVFV, RVFV-LMS-split, RVFV-LSS, RVFV-LMMS$_{NSs}$, RVFV-LMMS$_{eGFP}$, RVFV-LMMS$_{delNSs}$, and RVFV-LMMM genomes. The (NSm)GnGc gene was split at the first amino acid of the predicted signal sequence of Gc. (B) Plaque phenotypes of RVFV variants with segmented GPC genes were visualized by IFA. BSR cells were infected with an MOI of 0.01 to 0.001, fixed at 48 h postinfection, and evaluated for the presence of Gn antigen using monoclonal antibody 4-39-cc. For each virus a representative picture was taken.
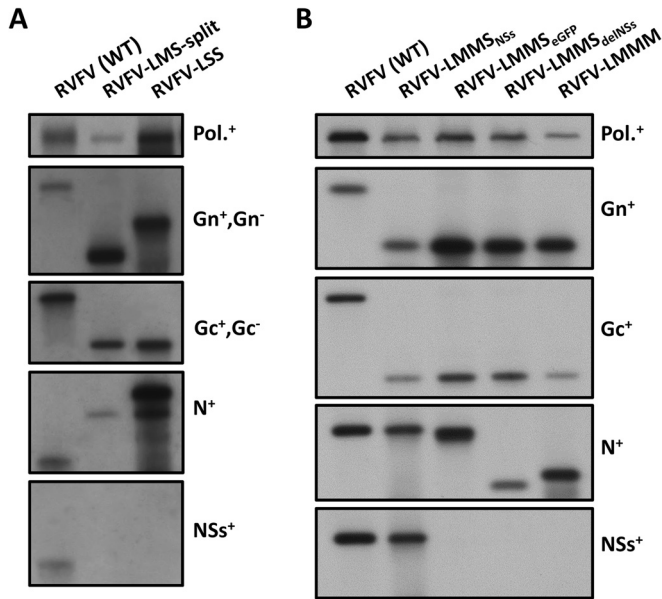
FIG 3 Confirmation of genotypes of RVFV variants with segmented GPC genes. (A and B) Northern blot analysis of RVFV, RVFV-LMS-split, and RVFV-LSS (A) and of RVFV-LMMS$_{NSs}$, RVFV-LMMS$_{eGFP}$, RVFV-LMMS$_{delNSs}$, and RVFV-LMMM (B). Viral RNA was isolated of passage 3 viral stocks using TRIzol-LS and RNA was separated in 1% agarose gels. After transfer of the RNA to nitrocellulose membranes, hybridizations were performed with probes recognizing the polymerase (Pol.), Gn, Gc, N, or NSs gene (see Table S2 in the supplemental material). The used probes are indicated at the right of each image. Superscripts: +, recognizes genomic-sense orientation; −, recognizes antigenic-sense orientation in wild-type virus.
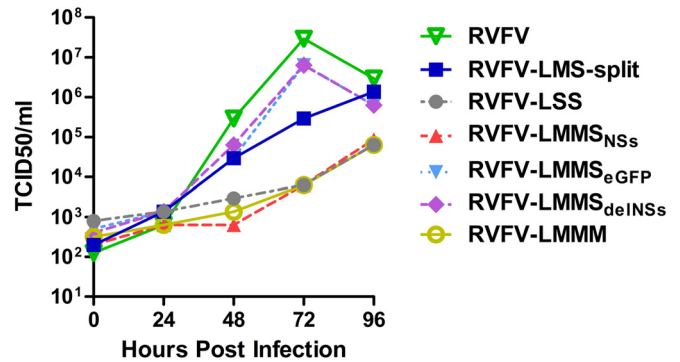

FIG 4 Growth curve of RVFV variants with segmented GPC genes. BSR cells were infected with RVFV variants at an MOI of 0.01. Titers were determined at the indicated time points by serial dilution of the supernatants on BSR cells, followed by IFA 48 h postinfection. The data represent the means of three experiments.

ing from RVFV-LSS infection was less pronounced and delayed. The ability to rescue RVFV-LSS confirms that RVFV is able to package more than one S segment into a single virion (35).

RVFV is able to maintain four genome segments. To further investigate RVFV genome packaging, we evaluated whether viruses could be constructed that maintain four instead of three genome segments (RVFV-4s); one L-, one S-, and two M-type segments. Rescue experiments were performed with transcription plasmids pUC57-L, pUC57-S-eGFP, pUC57-M-NSmGn, and pUC57-M-Gc. In this situation, the virus contains an authentic L segment, an S segment that encodes N and enhanced green fluorescent protein (eGFP), and two M-type segments that encode either NSmGn or Gc. In several attempts, again evidenced by IFA and Northern blotting (Fig. 2 and 3), the rescue of infectious four-segment RVFV was successful. The RVFV-4s eGFP variant, hereafter referred to as RVFV-LMMS$_{eGFP}$, is able to grow up to 10^7 TCID$_{50}$/ml in BSR cells (Fig. 4).

In addition to RVFV-LMMS$_{eGFP}$, we tried to rescue RVFV-4s variants with S segments expressing N and NSs or solely N. Rescue experiments were performed as described for RVFV-LMMS$_{eGFP}$, but instead of pUC57-S-eGFP, pUC57-S (encoding N and NSs) and pUC57-S-delNSs (encoding N) were used. Both viruses, here referred to as RVFV-LMMS$_{NSs}$ and RVFV-LMMS$_{delNSs}$, were viable and able to grow up to 10^6 and 10^7 TCID$_{50}$/ml in BSR cells, respectively (Fig. 2, 3, and 4). Like the other variants with a segmented GPC, RVFV-4s induced clear CPE about 1 day later than wild-type virus.

RVFV is able to maintain four genome segments, three of which are M-type segments. The results thus far strongly suggest

that RVFV genome packaging is relatively flexible. To further evaluate this flexibility, we tried to rescue a four-segment virus with three instead of two M-type genome segments. In this situation, NSmGn, Gc, and also N are all encoded by genome segments with M-type UTRs. Rescue experiments were performed with transcription plasmids pUC57-L, pUC57-M-NSmGn, pUC57-M-Gc, and pUC57-M-N. In several attempts, successful rescue of RVFV-LMMM could be confirmed by IFA and Northern blot analysis (Fig. 2 and 3), and the virus was able to grow up to 10^6 TCID$_{50}$/ml in BSR cells (Fig. 4). The ability to rescue RVFV-LMMM virus emphasizes that RVFV genome packaging, at least in mammalian cells, can be highly flexible.

Variations in intracellular protein expression after infection with RVFV variants containing segmented GPC genes. To evaluate whether the rescued RVFV variants express altered levels of Gn, Gc, or N compared to wild-type virus, we performed Western blot analysis of lysates of infected BSR cells (Fig. 5). The results show that expression of Gn and Gc from antigenic-sense RNA is generally lower than expression from genomic-sense RNA. For example, Gc expression in RVFV-LMS-split and Gn and Gc expression in RVFV-LSS infected cells is lower than the levels observed after infection with wild-type virus. The high expression of N in RVFV-LSS-infected cells can be explained by the presence of two copies of N in, respectively, the S-(N+NSmGn) and S-(N+Gc) segments. In contrast, the lower N expression in the RVFV-4s variants suggests that the presence of an additional M segment results in reduced transcription and translation of the S segment. Likely, the viral polymerase has higher affinity for M-type segments compared to S-type segments. Remarkably, despite reduced N expression, cells infected with four-segment viruses display increased expression of Gn. Since UTR sequences are similar for the M-NSmGn and M-Gc segments, we hypothesize that signals are present within the NSmGn-coding region that enhance transcription and/or replication by the polymerase. The reduced expression of Gc in RVFV-LMMM-infected cells compared to RVFV-LMMS-infected cells can be explained by an extra level of competition for polymerase proteins. The smaller size of the M segment encoding the N protein and the increased affinity of the polymerase for the M-UTR in combination with the NSmGn-
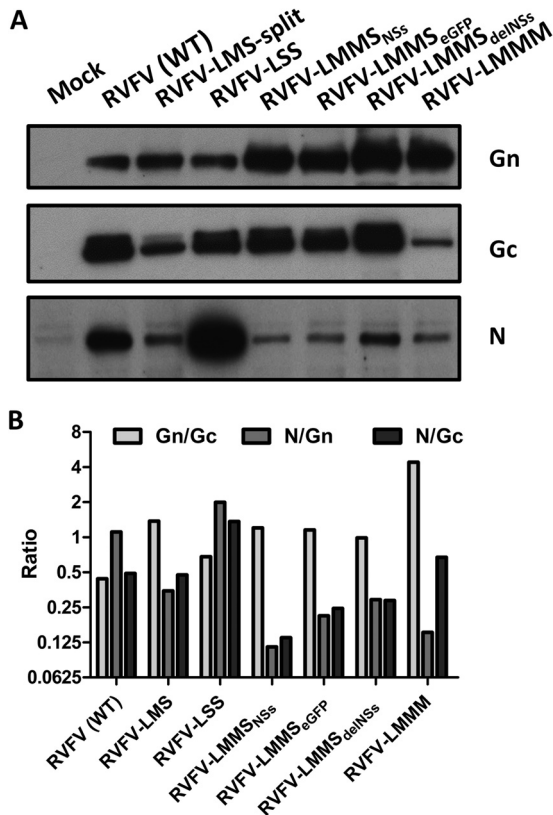
FIG 5 Viral protein expression in BSR cells infected with RVFV variants with segmented GPC genes. (A) BSR cells were infected at an MOI of 1 with the RVFV variants, and at 24 h postinfection the expression of Gn, Gc, and N was evaluated in cell lysates by Western blotting. (B) Viral protein ratios were determined by dividing band intensities. Intensities were determined using ImageQuant software (GE Healthcare Life Sciences). *, Due to low protein expression at 24 h postinfection, lysates of RVFV-LSS were taken 40 h postinfection.

coding region probably have negative effects on the replication and the expression of the M-type segment encoding Gc. Altogether, these results indicate that RVFV is able to cope with less balanced protein expression but suggests that a balanced expression is highly preferred.

Evidence for packaging of four genome segments into a single virion. To produce progeny virions, RVFV-4s must deliver all four genome segments into a single host cell. Theoretically, this can be achieved by infection with a single virion containing all four segments or, alternatively, by coinfection of complementing replicon particles, lacking at least one of the genome segments. To evaluate which of the two mechanisms is used by the RVFV-4s virus, we infected BSR cells with RVFV-LMMS$_{eGFP}$ and evaluated eGFP, Gn, and Gc expression at 16 h postinfection using IFA. Authentic RVFV expressing eGFP from the NSs location (RVFV$_{eGFP}$) was used as a reference. As expected, the vast majority (>90%) of RVFV$_{eGFP}$ virions contain at least one L, one M, and one S segment, as evidenced by the high percentage of infected cells that expressed eGFP, Gn, and Gc (Fig. 6). Infrequently, cells were observed that expressed eGFP in the absence of Gn and Gc. These cells were most likely infected by naturally occurring replicon particles lacking the M segment.

Comparable to RVFV$_{eGFP}$, almost all (>90%) eGFP-express-

ing cells showed expression of both Gn and Gc after infection with RVFV-LMMS$_{eGFP}$. Once again, only a limited number of eGFP-positive cells were observed that did not express Gn and Gc (Fig. 6). As expected, there were also some eGFP-positive cells that expressed Gn in the absence of Gc, or Gc in the absence of Gn, indicative for the presence of three-segmented replicons. These results, together with the observation that infection at a very low multiplicity of infection (MOI) of <0.001 resulted in foci of infection, suggest that RVFV-4s primarily produces progeny after infection by virions containing four genome segments, rather than by infection with complementing replicon particles.

Cellular localization of Gn and Gc in RVFV-4s-infected cells. To compare the cellular localization of Gn and Gc in RVFV-4s-infected cells to their localization in cells infected with wild-type virus, we infected BSR cells with RVFV-LMMS$_{eGFP}$ or RVFV$_{eGFP}$ and visualized Gn and Gc using IFA. Interestingly, Gn and Gc of the four-segmented viruses seemed to colocalized to the Golgi with equal efficiency as the corresponding proteins of the wild-type virus (Fig. 7). These results suggest that Gn and Gc interact efficiently, also when expressed from different genome segments.

Growth of RVFV with segmented GPC genes in insect cell culture. In the experiments described thus far, viruses with segmented GPC genes were grown in mammalian cells. Since RVFV is able to grow efficiently in insect cells, we compared the growth of wild-type and mutant viruses in *Aedes albopictus* C6/36 insect cell culture. As a positive control, viruses were grown in BSR cells. As expected, authentic RVFV was able to grow efficiently in the C6/36 cells. In sharp contrast, none of the viruses with segmented GPC genes was able to grow efficiently in C6/36 cell culture (Fig. 8). This result suggests that mechanisms of RVFV assembly and/or replication differ between mammalian and insect cells.

RVFV-4s is avirulent in mice. Since RVFV-4s displays reduced growth in mammalian cells and very limited spread in insect cells, we hypothesized that RVFV-4s is less able to cause disease. To study virulence, we evaluated whether RVFV-LMMS$_{NSs}$ is able to cause disease in a mouse model. Mice were infected with either a low ($10^{3.8}$ TCID$_{50}$) or a high ($10^{5.8}$ TCID$_{50}$) dose of RVFV-LMMS$_{NSs}$, and at 1, 4, 8, and 11 days postinfection mice were sacrificed for the evaluation of virus dissemination to the organs. As a positive control, one group of mice was infected with a low dose ($10^{2.8}$ TCID$_{50}$) of authentic RVFV. All mice infected with authentic RVFV died within 4 days postinfection, whereas none of the mice infected with RVFV-LMMS$_{NSs}$ died or showed clinical symptoms, not even when inoculated with the 500-fold higher dose (Fig. 9A). Evaluation of virus dissemination in the livers and brains at several time points confirmed that RVFV-LMMS$_{NSs}$ was unable to spread systemically (Fig. 9B). Altogether, these results demonstrate that RVFV-4s is avirulent in mice.

RVFV-4s induces a protective immune response in mice. Since RVFV-4s grows relatively well in cell culture and is avirulent in mice, we consider this virus a promising vaccine candidate. To investigate whether RVFV-4s is able to induce a protective immune response in mice, we performed a vaccination-challenge experiment. Mice were intramuscularly vaccinated with $10^{5.8}$ TCID$_{50}$ of RVFV-LMMS$_{eGFP}$ or RVFV-LMMS$_{delNSs}$. As a positive control, mice were vaccinated with $10^{5.8}$ TCID$_{50}$ NSR-Gn (29). At 3 weeks postvaccination, mice were challenged with a lethal dose of authentic RVFV. Within 4 days postchallenge all mock-vaccinated control mice succumbed to the infection (Fig. 10A). In contrast, mice vaccinated with RVFV-LMMS$_{eGFP}$ or RVFV-LMMS$_{delNSs}$ remained
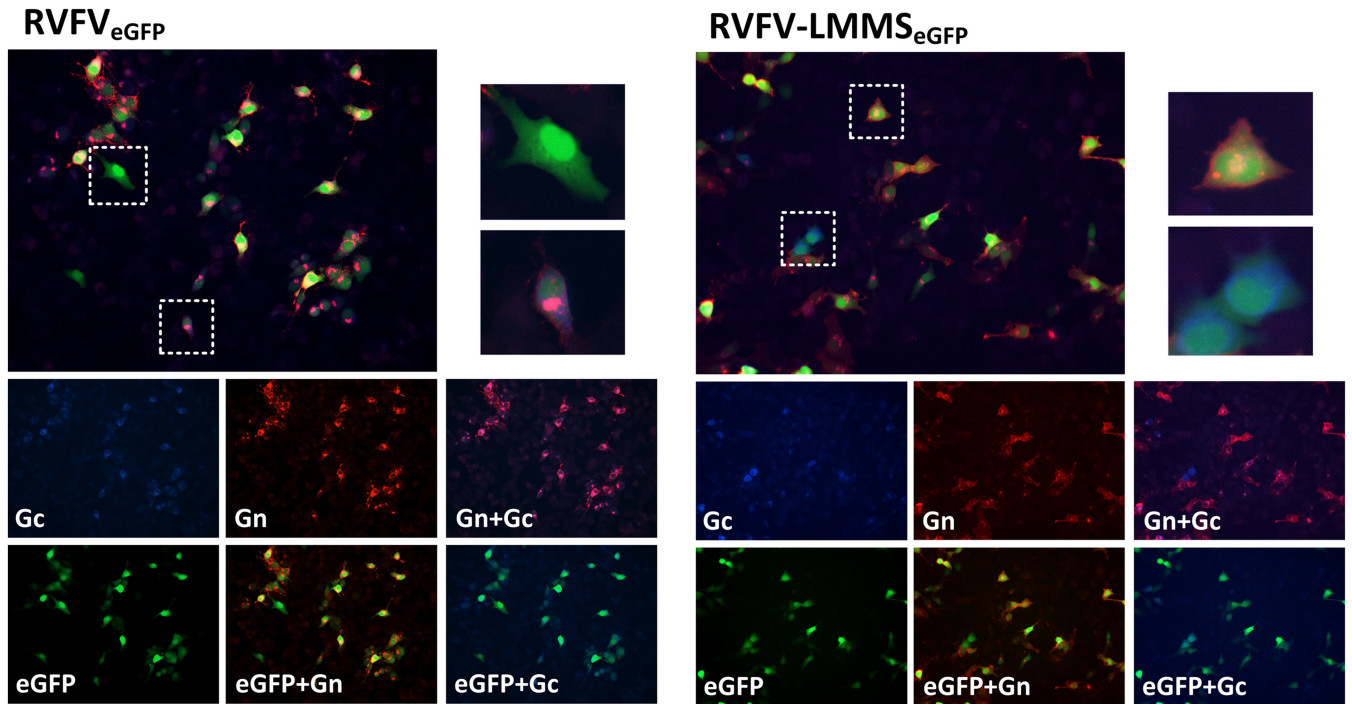
RVFV$_{eGFP}$

RVFV-LMMS$_{eGFP}$

FIG 6 Gn and Gc expression in RVFV$_{eGFP}$- and RVFV-LMMS$_{eGFP}$-infected cells. BSR cells were infected at an MOI of 0.1 with RVFV$_{eGFP}$ or RVFV-LMMS$_{eGFP}$, and at 16 h postinfection the cells were fixed and evaluated for Gn (red) and Gc (blue) expression using IFA. Pictures were taken using the EVOS-FL microscope with a ×10 objective lens.

healthy during the entire experiment. Analysis of sera and organs of vaccinated animals demonstrated the presence of a strong neutralizing antibody response (Fig. 10B) and the absence of systemic spread of challenge virus (Fig. 10C and D). Collectively, these results suggest that RVFV-4s is a vaccine candidate that optimally combines efficacy and safety.

DISCUSSION

Bunyaviruses express their surface proteins, which are essential for host-cell attachment and fusion, as a GPC. The proteolytic cleavage of the GPC by host proteases is an essential step in the maturation process. Using this strategy, most bunyaviruses are expected to maintain a constant ratio of 1:1 between their receptor-binding and fusion proteins. In RVFV, the receptor-binding protein Gn and the fusion protein Gc form heterodimers as building blocks for higher-order capsomers, which assemble into a T=12 icosahedral lattice (36, 37). Transient expression studies have demonstrated that expression of Gc in the absence of Gn results in Gc accumulation in the endoplasmic reticulum, whereas coexpression of Gn and Gc results in Golgi localization of both proteins (38–40). Our results expand on these previous studies by demonstrating that expression of Gn and Gc from two separate viral genome segments does not compromise their colocalization in the cell.

In wild-type virus, the Gc signal sequence (16 amino acids) is expected to be retained in the mature Gn protein (13, 14). In the present study, we segmented the GPC gene at the first amino acid of the signal sequence of Gc, resulting in a full-length Gc protein and a Gn protein with a truncated cytosolic tail that lacks the C-terminal membrane anchor. This strategy was chosen to prevent overlapping sequences that could theoretically facilitate a re-

combination event resulting in the formation of an intact GPC. We found it remarkable that truncation of the cytosolic tail of Gn does not prohibit particle assembly. However, we cannot exclude the possibility that RNP binding to the truncated cytosolic tail of Gn is somewhat compromised (22).

By analyzing Western blot data (Fig. 5), Northern blot results (Fig. 3), and the growth curves (Fig. 4), we obtained novel insights into the requirements for efficient RVFV growth and expanded our knowledge on RVFV genome packaging. For example, efficient formation of infectious virions seems to require high levels of expression of all structural proteins. Variants that showed greatly reduced expression of one or more viral proteins (like RVFV-LSS and RVFV-LMMM) were unable to grow to high titers. Regarding packaging, it was interesting to find that two four-segmented viruses (LMMS$_{delNSs}$ and LMMS$_{eGFP}$) replicated more efficiently than a virus with a three-segmented genome (LMS-split). The latter virus, which expresses NSmGn from the M segment and Gc from the S segment, was nonetheless readily rescued, whereas we did not succeed in rescuing a similar three-segmented virus in which the NSmGn and Gc genes are located in the opposite locations. The latter finding makes clear that optimal configuration of a reconfigured RVFV genome cannot easily be predicted and has to be determined empirically.

In addition to the RVFV variants characterized in the present study, we expect that several other variants, with rearranged coding and noncoding sequences can be created. Nevertheless, we envisage that segment rearrangements will generally result in viruses with lower overall fitness. In accordance to this assumption, rearrangements of coding and noncoding sequences were previously demonstrated to reduce the fitness of a member of the *Or-*
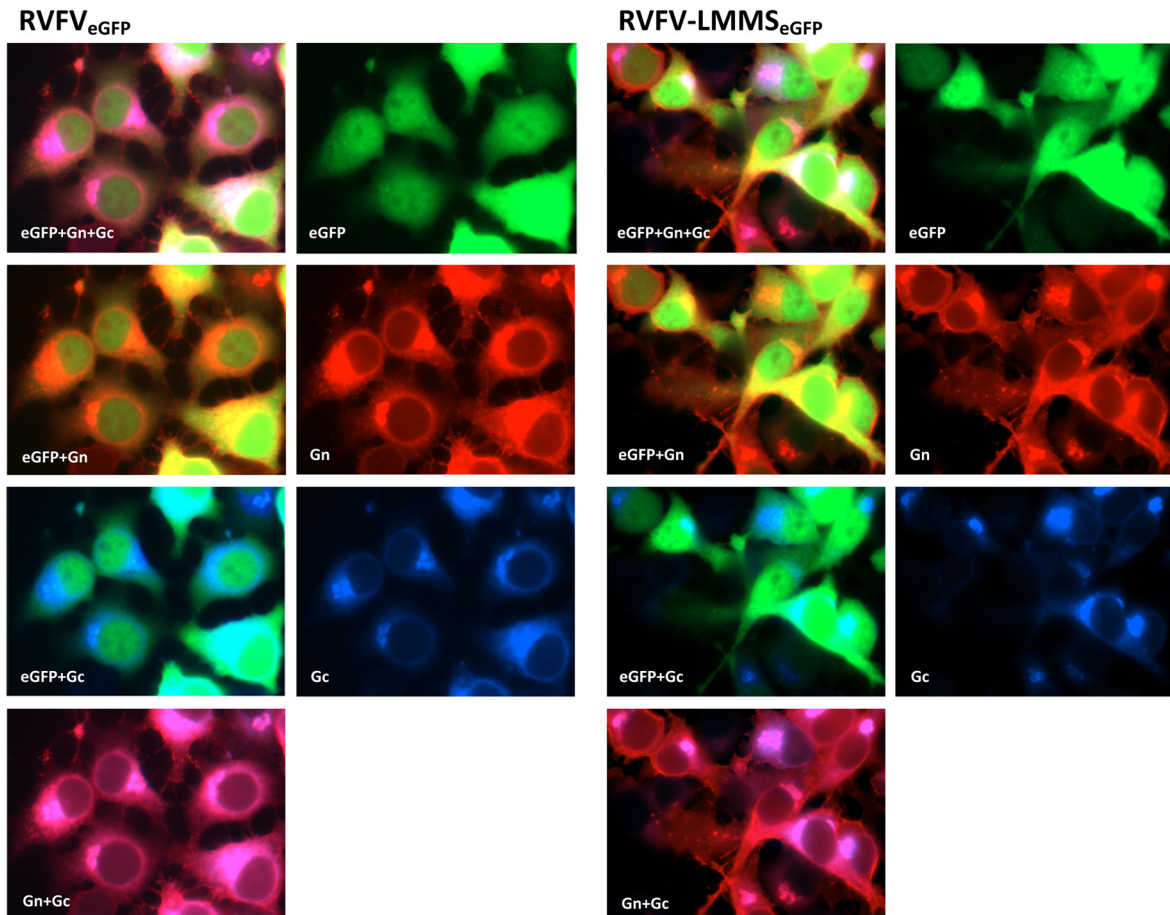
RVFV$_{eGFP}$

RVFV-LMMS$_{eGFP}$

FIG 7 Gn and Gc distribution in RVFV$_{eGFP}$- and RVFV-LMMS$_{eGFP}$-infected cells. BSR cells, grown on coverslips, were infected with an MOI of 0.5 with RVFV$_{eGFP}$ or RVFV-LMMS$_{eGFP}$. At 16 h postinfection the cells were fixed and evaluated for the presence of Gn (red) and Gc (blue) expression using IFA. Pictures were taken using the EVOS-FL microscope with a ×100 oil objective lens.

thobunyavirus genus. A Bunyamwera virus with M-type UTRs flanking the polymerase gene showed reduced growth in cultured cells and displayed reduced virulence in mice (41). In addition, a previously created RVFV with a two-segmented genome, which
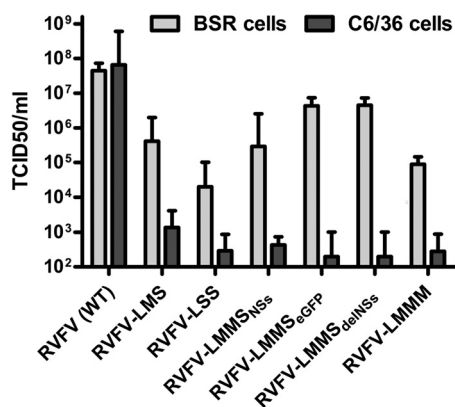

FIG 8 Growth of RVFV variants in insect cells. C6/36 cells and BSR cells were infected with the indicated RVFV variants at an MOI of 0.01. Supernatants were collected at 4 days postinfection and titrated on BSR cells. Bars represent means and standard errors of three experiments.

expresses the GPC gene from the NSs location of the S-segment, was shown to grow less efficiently in both mammalian and insect cell culture (25). In a very recent study the consequences of reconfiguring the ambisense S genome segment by swapping the N and NSs genes without changing the UTR sequences was investigated (42). Although this "swap" virus, as well as the viruses created in the present work, can be amplified efficiently in tissue culture, efficient growth was found to depend more strongly than in wild-type virus on cell type, MOI, and cell density.

Our results suggest that the RVFV-4s population mainly comprises virus particles that contain four genome segments, rather than replicon particles that depend on coinfection for the production of progeny virions. Nevertheless, this evidence is not conclusive. We are currently optimizing single-molecule pulldown (SiMPull) experiments combined with fluorescence *in situ* hybridization (FISH) to determine the genome composition of RVFV-4s virions. This approach was successfully used to demonstrate that influenza virus uses a highly selective genome packaging strategy (43).

After animal experiments demonstrated that RVFV-4s is completely avirulent and highly protective in the mouse model, the use of the RVFV-4s as a live-attenuated vaccine was considered. For this application, genetic stability upon passage of the virus in tis-
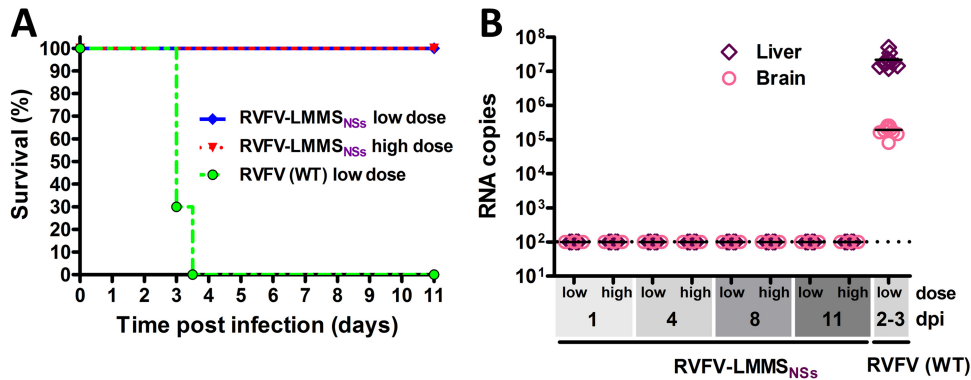
FIG 9 Virulence of RVFV-4s. (A) Survival curve of mice challenged with a high ($10^{5.8}$ TCID$_{50}$) or a low ($10^{3.8}$ TCID$_{50}$) dose of RVFV-LMMS$_{NSs}$. Control mice were challenged with a low ($10^{2.8}$ TCID$_{50}$) dose of authentic RVFV. (B) Virus dissemination in the livers and brains of mice euthanized at various times postinfection was determined by qRT-PCR. dpi, days postinfection.

sue culture is essential. To address this question, RVFV-LMMS$_{eGFP}$ and RVFV-LMMS$_{delNSs}$ were passaged 10 times in BSR cells and analyzed by Northern blotting. The results show that the S-type genome segment and both M-type genome segments (M-NSmGn and M-Gc) are stable maintained (see Fig. S1 in the supplemental material). In contrast, the L segment appeared to be less

stable, as evidenced by the presence of truncated RNAs. Most likely, multiply passage of RVFV-4s in BSR cells results in the accumulation of defective RNAs. The accumulation of defective RNAs of the L segment upon sequential passaging is commonly observed in bunyavirus research (44–46). Fortunately, we found that passage of the same viruses in Vero-E6 cells did not result in
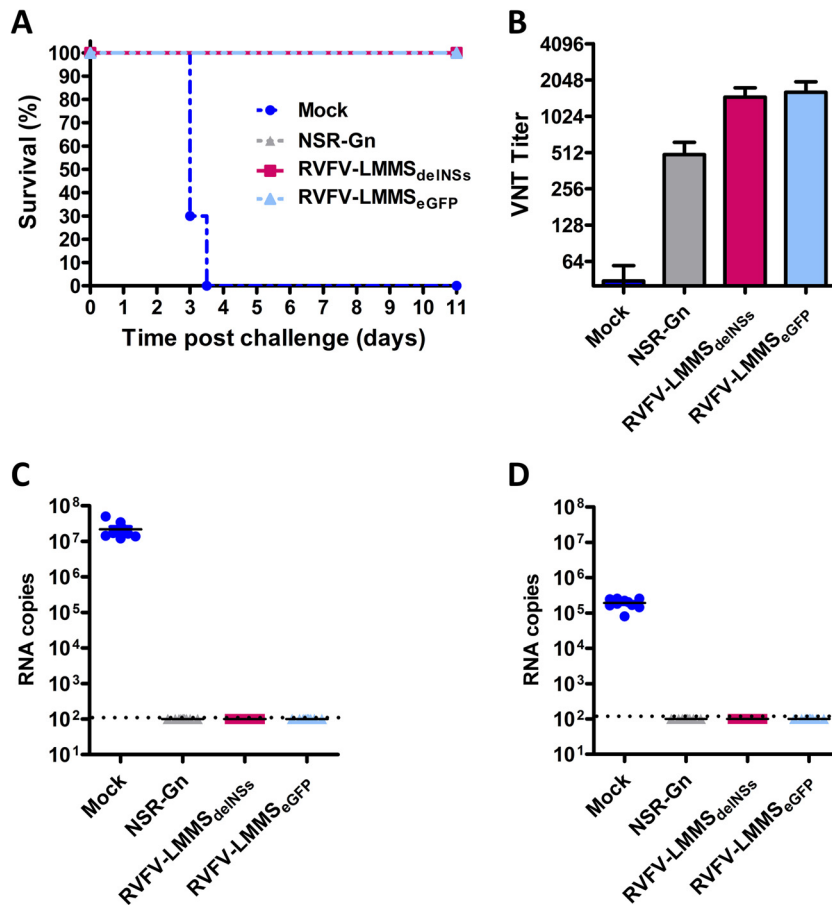

FIG 10 Vaccination-challenge experiment with RVFV-4s. (A) Survival curve of mice that were mock, NSR-Gn, RVFV-LMMS$_{eGFP}$, or RVFV-LMMS$_{delNSs}$ vaccinated. At 3 weeks postvaccination, mice were challenged with a lethal RVFV challenge dose. (B) RVFV neutralization titers present in sera the day before challenge. Virus dissemination to livers (C) and brains (D) was determined by qRT-PCR.

detectable levels of defective RNAs, and we have therefore selected these cells for future vaccine production.

The ability to construct bunyaviruses with segmented GPC genes may have significant implications for the development of next-generation vaccines based on live-attenuated viruses. The RVFV-4s viruses, for example, combine good *in vitro* growth with high *in vivo* efficacy and safety. Titers of up to 10^7 TCID$_{50}$/ml could be reached in mammalian cell culture, and mice could be fully protected by a single vaccination. It is important to note that the RVFV-4s virus is unique in being completely avirulent in the mouse model, even when containing all authentic genes from a highly virulent RVFV. However, because NSs does not contribute to vaccine efficacy and its absence further adds to the safety profile, we will make use of RVFV-4s viruses lacking the NSs gene for further vaccine safety and efficacy studies in the natural target species.

As said, the results of the present work, as well as those of earlier studies, demonstrate a certain level of plasticity in RVFV packaging. Altogether, we expect that RVFV does not exclusively use a selective or random genome packaging strategy. The ability to package two or even three genome segments with identical UTRs in a single virion suggests a more random packaging mechanism, whereas the reduced growth and reduced virulence of the RVFV-4s viruses suggests a preference for selective packaging. We hypothesize that the flexibility observed in RVFV genome packaging might be a feature of other bunyaviruses as well and could explain the ability of these viruses to package antigenomic RNA into virions (35, 42). Notably, the differences in growth of the RVFV variants with segmented GPC genes in mammalian versus mosquito cells points to mechanistic differences in glycoprotein processing and/or to a more selective genome packaging in mosquito cells. The latter may explain the increased infectivity of mosquito cell-derived RVFV compared to mammalian cell-derived virus (47).

Collectively, splitting of the RVFV GPC gene has provided a novel and very helpful approach for studying bunyavirus genome packaging and offers new possibilities for the development of next-generation live-attenuated bunyavirus vaccines.

ACKNOWLEDGMENTS

REFERENCES

1. **Pepin M, Bouloy M, Bird BH, Kemp A, Paweska J.** 2010. Rift Valley fever virus (*Bunyaviridae*: *Phlebovirus*): an update on pathogenesis, molecular epidemiology, vectors, diagnostics and prevention. Vet. Res. **41:**61. http://dx.doi.org/10.1051/vetres/2010033.
2. **Elliott RM.** 1997. Emerging viruses: the *Bunyaviridae*. Mol. Med. **3:**572–577.
3. **Ikegami T, Narayanan K, Won S, Kamitani W, Peters CJ, Makino S.** 2009. Rift Valley fever virus NSs protein promotes posttranscriptional downregulation of protein kinase PKR and inhibits eIF2α phosphorylation. PLoS Pathog. **5:**e1000287. http://dx.doi.org/10.1371/journal.ppat.1000287.
4. **Ikegami T, Narayanan K, Won S, Kamitani W, Peters CJ, Makino S.** 2009. Dual functions of Rift Valley fever virus NSs protein: inhibition of host mRNA transcription and post-transcriptional downregulation of protein kinase PKR. Ann. N. Y. Acad. Sci. **1171**(Suppl 1)**:**E75–E85. http://dx.doi.org/10.1111/j.1749-6632.2009.05054.x.
5. **Billecocq A, Spiegel M, Vialat P, Kohl A, Weber F, Bouloy M, Haller O.** 2004. NSs protein of Rift Valley fever virus blocks interferon production by inhibiting host gene transcription. J. Virol. **78:**9798–9806. http://dx.doi.org/10.1128/JVI.78.18.9798-9806.2004.
6. **Bouloy M, Janzen C, Vialat P, Khun H, Pavlovic J, Huerre M, Haller O.** 2001. Genetic evidence for an interferon-antagonistic function of rift valley fever virus nonstructural protein NSs. J. Virol. **75:**1371–1377. http://dx.doi.org/10.1128/JVI.75.3.1371-1377.2001.
7. **Muller R, Saluzzo JF, Lopez N, Dreier T, Turell M, Smith J, Bouloy M.** 1995. Characterization of clone 13, a naturally attenuated avirulent isolate of Rift Valley fever virus, which is altered in the small segment. Am. J. Trop. Med. Hyg. **53:**405–411.
8. **Won S, Ikegami T, Peters CJ, Makino S.** 2007. NSm protein of Rift Valley fever virus suppresses virus-induced apoptosis. J. Virol. **81:**13335–13345. http://dx.doi.org/10.1128/JVI.01238-07.
9. **Terasaki K, Won S, Makino S.** 2013. The C-terminal region of Rift Valley fever virus NSm protein targets the protein to the mitochondrial outer membrane and exerts antiapoptotic function. J. Virol. **87:**676–682. http://dx.doi.org/10.1128/JVI.02192-12.
10. **Kading RC, Crabtree MB, Bird BH, Nichol ST, Erickson BR, Horiuchi K, Biggerstaff BJ, Miller BR.** 2014. Deletion of the NSm virulence gene of Rift Valley fever virus inhibits virus replication in and dissemination from the midgut of *Aedes aegypti* mosquitoes. PLoS Negl. Trop. Dis. **8:**e2670. http://dx.doi.org/10.1371/journal.pntd.0002670.
11. **Weingartl HM, Zhang S, Marszal P, McGreevy A, Burton L, Wilson WC.** 2014. Rift Valley fever virus incorporates the 78-kDa glycoprotein into virions matured in mosquito C6/36 cells. PLoS One **9:**e87385. http://dx.doi.org/10.1371/journal.pone.0087385.
12. **Collett MS, Purchio AF, Keegan K, Frazier S, Hays W, Anderson DK, Parker MD, Schmaljohn C, Schmidt J, Dalrymple JM.** 1985. Complete nucleotide sequence of the M RNA segment of Rift Valley fever virus. Virology **144:**228–245. http://dx.doi.org/10.1016/0042-6822(85)90320-4.
13. **Suzich JA, Kakach LT, Collett MS.** 1990. Expression strategy of a phlebovirus: biogenesis of proteins from the Rift Valley fever virus M segment. J. Virol. **64:**1549–1555.
14. **Gerrard SR, Nichol ST.** 2007. Synthesis, proteolytic processing and complex formation of N-terminally nested precursor proteins of the Rift Valley fever virus glycoproteins. Virology **357:**124–133. http://dx.doi.org/10.1016/j.virol.2006.08.002.
15. **Guu TSY, Zheng WJ, Tao YZJ.** 2012. Bunyavirus: structure and replication. Adv. Exp. Med. Biol. **726:**245–266. http://dx.doi.org/10.1007/978-1-4614-0980-9_11.
16. **Gauliard N, Billecocq A, Flick R, Bouloy M.** 2006. Rift Valley fever virus noncoding regions of L, M, and S segments regulate RNA synthesis. Virology **351:**170–179. http://dx.doi.org/10.1016/j.virol.2006.03.018.
17. **Flick K, Katz A, Overby A, Feldmann H, Pettersson RF, Flick R.** 2004. Functional analysis of the noncoding regions of the Uukuniemi virus (*Bunyaviridae*) RNA segments. J. Virol. **78:**11726–11738. http://dx.doi.org/10.1128/JVI.78.21.11726-11738.2004.
18. **Kohl A, Lowen AC, Leonard VH, Elliott RM.** 2006. Genetic elements regulating packaging of the Bunyamwera orthobunyavirus genome. The J. Gen. Virol. **87:**177–187. http://dx.doi.org/10.1099/vir.0.81227-0.
19. **Overby AK, Popov V, Neve EP, Pettersson RF.** 2006. Generation and analysis of infectious virus-like particles of Uukuniemi virus (*Bunyaviridae*): a useful system for studying bunyaviral packaging and budding. J. Virol. **80:**10428–10435. http://dx.doi.org/10.1128/JVI.01362-06.
20. **Terasaki K, Murakami S, Lokugamage KG, Makino S.** 2011. Mechanism of tripartite RNA genome packaging in Rift Valley fever virus. Proc. Natl. Acad. Sci. U. S. A. **108:**804–809. http://dx.doi.org/10.1073/pnas.1013155108.
21. **Murakami S, Terasaki K, Narayanan K, Makino S.** 2012. Roles of the coding and noncoding regions of Rift Valley fever virus RNA genome segments in viral RNA packaging. J. Virol. **86:**4034–4039. http://dx.doi.org/10.1128/JVI.06700-11.
22. **Piper ME, Sorenson DR, Gerrard SR.** 2011. Efficient cellular release of Rift Valley fever virus requires genomic RNA. PLoS One **6:**e18070. http://dx.doi.org/10.1371/journal.pone.0018070.
23. **Kortekaas J, Oreshkova N, Cobos-Jimenez V, Vloet RP, Potgieter CA, Moormann RJ.** 2011. Creation of a nonspreading Rift Valley fever virus. J. Virol. **85:**12622–12630. http://dx.doi.org/10.1128/JVI.00841-11.
24. **Dodd KA, Bird BH, Metcalfe MG, Nichol ST, Albarino CG.** 2012. Single-dose immunization with virus replicon particles confers rapid ro-

bust protection against Rift Valley fever virus challenge. J. Virol. **86:**4204–4212. http://dx.doi.org/10.1128/JVI.07104-11.

25. **Brennan B, Welch SR, McLees A, Elliott RM.** 2011. Creation of a recombinant Rift Valley fever virus with a two-segmented genome. J. Virol. **85:**10310–10318. http://dx.doi.org/10.1128/JVI.05252-11.

26. **Buchholz UJ, Finke S, Conzelmann KK.** 1999. Generation of bovine respiratory syncytial virus (BRSV) from cDNA: BRSV NS2 is not essential for virus replication in tissue culture, and the human RSV leader region acts as a functional BRSV genome promoter. J. Virol. **73:**251–259.

27. **Barnard BJ.** 1979. Rift Valley fever vaccine–antibody and immune response in cattle to a live and an inactivated vaccine. J. South Afr. Vet. Assoc. **50:**155–157.

28. **Das SC, Baron MD, Skinner MA, Barrett T.** 2000. Improved technique for transient expression and negative strand virus rescue using fowlpox T7 recombinant virus in mammalian cells. J. Virol. Methods **89:**119–127. http://dx.doi.org/10.1016/S0166-0934(00)00210-X.

29. **Oreshkova N, van Keulen L, Kant J, Moormann RJ, Kortekaas J.** 2013. A single vaccination with an improved nonspreading rift valley Fever virus vaccine provides sterile immunity in lambs. PLoS One **8:**e77461. http://dx.doi.org/10.1371/journal.pone.0077461.

30. **Keegan K, Collett MS.** 1986. use of bacterial expression cloning to define the amino-acid-sequences of antigenic determinants on the G2-glycoprotein of Rift Valley fever virus. J. Virol. **58:**263–270.

31. **de Boer SM, Kortekaas J, Spel L, Rottier PJ, Moormann RJ, Bosch BJ.** 2012. Acid-activated structural reorganization of the Rift Valley fever virus gC fusion protein. J. Virol. **86:**13642–13652. http://dx.doi.org/10.1128/JVI.01973-12.

32. **Kortekaas J, de Boer SM, Kant J, Vloet RP, Antonis AF, Moormann RJ.** 2010. Rift Valley fever virus immunity provided by a paramyxovirus vaccine vector. Vaccine **28:**4394–4401. http://dx.doi.org/10.1016/j.vaccine.2010.04.048.

33. **Martin-Folgar R, Lorenzo G, Boshra H, Iglesias J, Mateos F, Borrego B, Brun A.** 2010. Development and characterization of monoclonal antibodies against Rift Valley fever virus nucleocapsid protein generated by DNA immunization. Mabs-Austin **2:**275–284. http://dx.doi.org/10.4161/mabs.2.3.11676.

34. **Kortekaas J, Antonis AF, Kant J, Vloet RP, Vogel A, Oreshkova N, de Boer SM, Bosch BJ, Moormann RJ.** 2012. Efficacy of three candidate Rift Valley fever vaccines in sheep. Vaccine **30:**3423–3429. http://dx.doi.org/10.1016/j.vaccine.2012.03.027.

35. **Ikegami T, Won S, Peters CJ, Makino S.** 2005. Rift Valley fever virus NSs mRNA is transcribed from an incoming antiviral-sense S RNA segment. J. Virol. **79:**12106–12111. http://dx.doi.org/10.1128/JVI.79.18.12106-12111.2005.

36. **Freiberg AN, Sherman MB, Morais MC, Holbrook MR, Watowich SJ.** 2008. Three-dimensional organization of Rift Valley fever virus revealed by cryoelectron tomography. J. Virol. **82:**10341–10348. http://dx.doi.org/10.1128/JVI.01191-08.

37. **Huiskonen JT, Overby AK, Weber F, Grunewald K.** 2009. Electron cryo-microscopy and single-particle averaging of Rift Valley fever virus: evidence for GN-GC glycoprotein heterodimers. J. Virol. **83:**3762–3769. http://dx.doi.org/10.1128/JVI.02483-08.

38. **Carnec X, Ermonval M, Kreher F, Flamand M, Bouloy M.** 2014. Role of the cytosolic tails of Rift Valley fever virus envelope glycoproteins in viral morphogenesis. Virology **448:**1–14. http://dx.doi.org/10.1016/j.virol.2013.09.023.

39. **Gerrard SR, Nichol ST.** 2002. Characterization of the Golgi retention motif of Rift Valley fever virus G(N) glycoprotein. J. Virol. **76:**12200–12210. http://dx.doi.org/10.1128/JVI.76.23.12200-12210.2002.

40. **Matsuoka Y, Chen SY, Compans RW.** 1994. A signal for Golgi retention in the bunyavirus G1 glycoprotein. J. Biol. Chem. **269:**22565–22573.

41. **Lowen AC, Boyd A, Fazakerley JK, Elliott RM.** 2005. Attenuation of bunyavirus replication by rearrangement of viral coding and noncoding sequences. J. Virol. **79:**6940–6946. http://dx.doi.org/10.1128/JVI.79.11.6940-6946.2005.

42. **Brennan B, Welch SR, Elliott RM.** 2014. The consequences of reconfiguring the ambisense s genome segment of rift valley Fever virus on viral replication in mammalian and mosquito cells and for genome packaging. PLoS Pathog. **10:**e1003922. http://dx.doi.org/10.1371/journal.ppat.1003922.

43. **Chou YY, Vafabakhsh R, Doganay S, Gao Q, Ha T, Palese P.** 2012. One influenza virus particle packages eight unique viral RNAs as shown by FISH analysis. Proc. Natl. Acad. Sci. U. S. A. **109:**9101–9106. http://dx.doi.org/10.1073/pnas.1206069109.

44. **Inoue-Nagata AK, Kormelink R, Sgro JY, Nagata T, Kitajima EW, Goldbach R, Peters D.** 1998. Molecular characterization of tomato spotted Wilt virus defective interfering RNAs and detection of truncated L proteins. Virology **248:**342–356. http://dx.doi.org/10.1006/viro.1998.9271.

45. **Marchi A, Nicoletti L, Accardi L, Di Bonito P, Giorgi C.** 1998. Characterization of Toscana virus-defective interfering particles generated in vivo. Virology **246:**125–133. http://dx.doi.org/10.1006/viro.1998.9195.

46. **Patel AH, Elliott RM.** 1992. Characterization of Bunyamwera virus defective interfering particles. J. Gen. Virol. **73**(Pt 2):389–396. http://dx.doi.org/10.1099/0022-1317-73-2-389.

47. **Nfon CK, Marszal P, Zhang S, Weingartl HM.** 2012. Innate immune response to Rift Valley fever virus in goats. PLoS Negl. Trop. Dis. **6:**e1623. http://dx.doi.org/10.1371/journal.pntd.0001623.